

# PETROLOGY OF NORTHWEST AFRICA 11515: MG-SUITE AND FAN SUITE BRECCIA

Y. Li<sup>1,2</sup>, P.J.A. McCausland<sup>1,2</sup>, R.L. Flemming<sup>1,2</sup>, <sup>1</sup>Department of Earth Sciences and <sup>2</sup>Institute for Earth and Space Exploration, Western University, London, ON, Canada N6A 5B7. [yli2889@uwo.ca](mailto:yli2889@uwo.ca)

**Introduction:** The proto-moon is thought to have been a wholly or largely molten body formed as the result of the Giant Impact between a Mars-sized body and proto-Earth [1,2]. The current lunar magmatism model, known as Lunar Magma Ocean (LMO), was developed largely based on the petrology and geochemistry discoveries made from Apollo samples [2-3]. Mafic minerals such as olivine and orthopyroxene are believed to have crystallized from the magma ocean to form the mantle, while a less dense ferroan-anorthositic (FAN) suite floated on the dense residual melt, forming the lunar crust. Denser residual material trapped between mantle and crust became enriched in incompatible elements as well as heavy elements such as Ti, leading to a mantle overturn, initiating secondary magmatism which formed a magnesian-rich rock suite (Mg-suite) [2-3]. Lunar meteorites, unlike returned samples, are from unknown locations on the moon which may include the far side, which is poorly studied by current missions [4-6]. Lunar meteorite Northwest Africa (NWA) 11515 provides a unique opportunity to study the petrology of the moon beyond that provided by returned samples.

NWA 11515 has been reported as a hybrid felspathic breccia in previous work [7]. In this study, we provide detailed petrologic study by X-ray diffraction and electron microprobe. We compare our results with literature data including both meteorites and returned samples, and we confirm the hybrid nature of the meteorite NWA 11515 breccia, resembling the mineralogy from both the Mg-suite and FAN suite. We also use a preliminary bytownite shock calibration curve [8] with quantitatively measured strain-related mosaicity (SRM) to constrain clast shock history.

**Methods:** Micro texture and mineral chemistry was determined by Electron Probe Microanalysis (EPMA) at Western University using a JEOL JXA-8530F field-emission electron microprobe with 5 wavelength dispersive spectrometers (WDS) proving a quantitative chemical analysis for major elements. Strain-related mosaicity (SRM) was measured by a Bruker D8 Discover  $\mu$ XRD at Western with a Co K $\alpha$  X-ray source ( $\lambda$  Co K $\alpha_1$  = 1.78897 Å) and Vantec-500 detector, with General Area Detector Diffraction System (GADDS) software, which obtains 2D diffraction patterns similar to Debye-Scherrer film. SRM analysis reflects the degree of misorientation in non-uniformly strained crystals [9-10]. Quantitative SRM analysis is done by Best Fit for Complex Peaks, a Matlab®-based program [11]. Shock pressure is constrained by observations on feldspar, with reference to a preliminary shock calibration curve developed on experimentally shocked bytownite [8, 12].

**Results:** Dominant silicate mineral phases in NWA 11515 are: Ca-rich plagioclase, low-Ca pyroxene, high-

Ca pyroxene, and olivine. Anorthite clasts have uniform composition of An $96.4 \pm 0.7$  (n = 52), however the morphology of the anorthite is variable: 1) large single clast, 2) granulitic anorthite with pyroxene and/or olivine; 3) acicular symplectite-like intergrowth with augite; 4) very-fine grained (powdered) mixture with mafic minerals such as olivine and pyroxene.

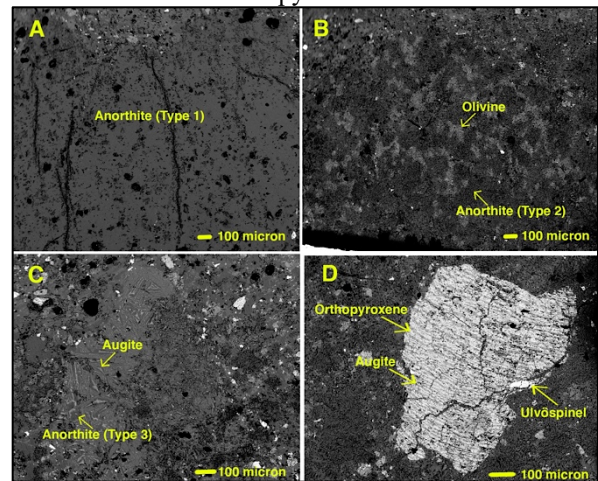


**Figure 1. Selected BSE image of clasts in NWA 11515.** 1A is Type 1 large angular anorthite clast; 1B is granulitic anorthite (Type 2 anorthite) with olivine shown as troctolitic clasts; 1C is intergrowth of augite and anorthite showing symplectite-like texture; 1D is augite and orthopyroxene exsolution lamellae with a chromium ulvöspinel.

Most olivine in this rock is seen as granulitic textures with anorthite and pyroxene resembling noritic-troctolitic clasts (Type 2) (Fig. 1B). Olivine is unlikely to have crystallized from a single source as they show large variation in magnesium content. Magnesian olivine clasts have mg# > 80, and more ferroan olivine clasts have mg# 60 to 64. Very ferroan olivine clasts (mg# 46 to 58) are rare. Pyroxene also shows large variation of Ca from Wo $2.9$  to Wo $44.8$ . One porphyritic pyroxene clast is found, bearing exsolution lamellae of orthopyroxene (En $43$  Fs $53$  Wo $4$ ) and augite (En $34$  Fs $27$  Wo $39$ ) (Fig. 1D). The spinel group mineral chromite is the major oxide present, appearing as inclusions in silicate minerals. However, the composition of chromite shows large variation of Ti abundance and relative amount of Al $_2$ O $_3$  and Cr $_2$ O $_3$ . Rare Cr-ulvöspinel (FeO wt%=50.3, TiO $_2$  wt%=23.8, Cr $_2$ O $_3$  wt%=17.5) appeared as an inclusion in the pyroxene clast showing orthopyroxene-augite exsolution lamellae (Fig. 1D). The composition is similar to the ulvöspinel found in Apollo 14 [13]. Low Ti (TiO $_2$  wt% of 1.9 to 6.2) chromite is common, however, with the relative abundance of Al $_2$ O $_3$  and Cr $_2$ O $_3$  varying: chromite in noritic-troctolitic clasts has Al $_2$ O $_3$  wt% of 12.5 to 14.3; chromite found as inclusions in the porphyritic olivine clast has Al $_2$ O $_3$  wt% of 6.8. A

very low titanium and high refractory spinel ( $\text{TiO}_2$  wt%=0.86 and  $\text{Al}_2\text{O}_3$  wt%=46.5) is also found as an inclusion in a large angular anorthite clast, which may represent primitive material crystallized from the lunar magma ocean. The observation of composition-invariant anorthite with varying mg# of coexisting mafic clasts is considered a characteristic of FAN-suite rocks [14]. Variation in mg# indicates the precursor anorthosites of the breccia may not have crystallized from a common magma, suggesting more complex igneous processes than a single LMO [14]. Regional melting of different parent rocks may be required to explain varied olivine and pyroxene compositions.

The molar ratio of mg# for mafic clasts versus An# for plagioclase (Fig. 2) shows a divergence of clasts into Mg-rich suite and FAN suite, with a similar trend toward granulites as in Allan Hills A81005 [6]. ALHA81005 is reported as a Mg-rich but completely KREEP-depleted breccia that cannot be explained by the LMO model, and it may represent the missing lithology not yet discovered by sample return missions [3]. Trace element analysis is needed to determine the geochemical affinity of NWA 11515 to KREEP and to conclude if it is also a KREEP-depleted troctolitic breccia.

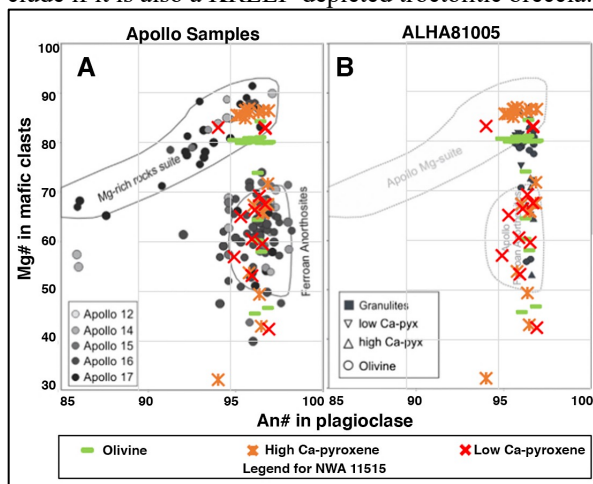


**Figure 2. Comparison of NWA 11515 to literature: Apollo samples and ALHA81005.** Plots [6] of Mg# molar ratio of  $100 \times \text{Mg}/(\text{Mg}+\text{Fe})$  in the mafic clasts versus An# as  $100 \times \text{Ca}/(\text{Ca}+\text{Na})$  in the plagioclase associated with mafic clasts. NWA 11515 (this study, colored symbols) shows the mixing lithology of both Mg-suite and FAN suite that were identified in Apollo samples and is similar to ALHA81005, which is Mg-rich but shows no KREEP components [6].

Figure 3 shows 2D-XRD patterns for four types of anorthite clasts. Type 2 anorthite clasts in NWA 11515 show mosaic spread along the chi-direction indicating misoriented subdomains in the strained crystal due to the destructive effects of shock (Fig 2B). Quantitative SRM analysis are obtained on Type 2 clasts yielding  $\Sigma(\text{FWHM}_\chi)$  of  $9.44^\circ \pm 2.69^\circ$  ( $n=6$ ) with pressure of  $25.8 \pm 6.5 \text{ GPa}$  with reference to the preliminary bytownite calibration curve in [8].

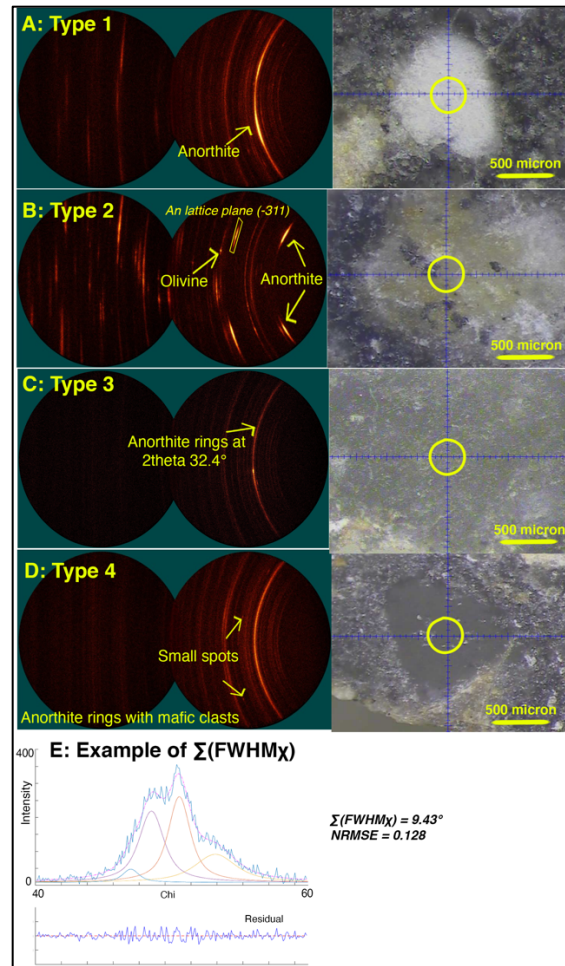


**Figure 3. 2D-XRD of four types of anorthite clasts and example of measuring SRM.** 3A to 3D show four anorthite clasts examined in this study. Left images show the 2D XRD pattern as bright diffraction intensity spots, streaks and rings; right images show target area with 300 µm X-ray beam size. In 3B, diffraction streaks are anorthite and spots are olivine. 3E shows the example of measuring SRM (yellow box in 3B) with Best Fit for Complex Peaks [11].

**References:** [1] Canup and Asphaug (2001) Nat. 412, 708–712 [2] Tanton et al. (2002) EPSL: 196 (3–4), 239–249. [3] Gross et al. (2020) JGR–Planets, 125 (5). e2019JE006225. [4] Lucey et al., (2006) Rev. Min. & Geo. 60, 83–219. [5] Roberts et al., (2019) MAPS, 54 (12), 3018–3035. [6] Gross et al. (2014) EPSL: 388, 318–328. [7] Li et al., (2020) LPSC Abs#2326. [8] Li et al., 2022 LPSC Abs#2095 [9] Flemming (2007) CJES, 44, 1333–1346. [10] Hörz and Quaide (1973) The Moon, 6, 45–82. [11] Li et al., (2020) Comp&Geosci, 144, 104572. [12] Jaret et al., (2018) JGR–Planets, 123 (7), 1701–1722. [13] El Goresy et al., (1971) EPSL, 13 (1), 121–129. [14] Korotev and Ivring (2021) MAPS, 56 (2), 206–240.

**Acknowledgement:** PJAM and RLF acknowledge continued research funding support from the NSERC – Discovery Grants program.